Materials Science & Engineering A 674 (2016) 98–103

Contents lists available at ScienceDirect

Materials Science & Engineering A

journal homepage: www.elsevier.com/locate/msea

Scale dependence of the strain rate sensitivity of Twinning-Induced Plasticity steel

A. Bintu [a], G.T. Vincze [a], R.C. Picu [b,*], A.B. Lopes [c], I. Bdikin [a]

[a] TEMA, Department of Mechanical Engineering, University of Aveiro, Campus Universitário de Santiago, 3810-193, Portugal
[b] Department of Mechanical, Aerospace and Nuclear Engineering, Rensselaer Polytechnic Institute, Troy, NY 12180, USA
[c] CICECO, Department of Materials and Ceramic Engineering, University of Aveiro, Campus Universitário de Santiago, 3810-193, Portugal

ARTICLE INFO

Article history:
Received 22 January 2016
Received in revised form
20 June 2016
Accepted 31 July 2016
Available online 1 August 2016

Keywords:
TWIP steel
Strain rate sensitivity
Nano-indentation
Deformation twinning

ABSTRACT

We report that the mechanical behavior of Twinning-Induced Plasticity steel deformed at different strain rates depends on the scale of observation. Slower-deformed samples have a higher twin density, which leads to larger flow stress measured in a macroscopic uniaxial test. When probed at the nanoscale by nano-indentation, samples pre-deformed at smaller strain rates exhibit systematically smaller hardness than samples pre-deformed at higher rates. The hardness-based nanoscale strain rate sensitivity is positive. The strain rate sensitivity measured by micro-hardness shifts to negative values as the indenter size and the probed volume increase. The effect is linked to the dislocation-twin interaction mechanism.

1. Introduction

Twinning-Induced Plasticity (TWIP) steels form a relatively new class of materials with exceptional strength and toughness. Most members of this family have ultimate tensile strength in the range 1.3–1.5 GPa and significant ductility, with strains at failure above 0.3 (30%), which entails large energy absorption before failure [1]. The yield stress is not exceptionally high, but TWIP steels exhibit large and almost strain-independent strain hardening which insures the stability of the deformation. These exceptional properties are due to the TWIP effect which amounts to a close correlation between dislocation activity and twinning during deformation [2–4]. Twins are usually considered obstacles to dislocation motion since twin boundaries are strong obstacles to dislocations moving on glide planes intersecting them. Hence, increasing twin density leads to a reduction of the mean free path for dislocations and consequently an increase of the flow stress. On the other hand, twinning dislocations may move freely along twin boundaries, which leads to an increase of the twin thickness. The competition between these two mechanisms, correlated with the low barrier for twin formation, leads to the observed exceptional properties of these steels [5].

Some TWIP steels exhibit negative strain rate sensitivity (SRS), and this is particularly pronounced at larger strains where strain localization may occur [6,7], leading to an apparent Portevin-Le-Chatelier effect characterized by serrations of the stress-strain curve [8]. This behavior has attracted some attention recently since strain localization reduces formability.

A large effort has been made over the last decade to understand the physical basis of the TWIP behavior e.g. [9–12]. Barbier et al. characterized the twinning microstructure in fine-grained 22 Mn–0.6C TWIP steels by electron backscatter diffraction (EBSD) and found that as the texture strengthens with the deformation, a strong $<111>$ orientation dependence of twinning is observed [13]. TEM investigation of the twinning deformation mechanism indicates stair-rod cross-slip as a mechanism for twin nucleation, especially in presence of stacking faults distributed within the grains which could act as preferential sites for the operation of this mechanism [14]. Most of the studies cited focus on the global deformation of TWIP. The correlation of global and local deformation should lead to further insight into the nature and operation of the fundamental mechanisms. An example of this nature is the work on Ni-enriched austenitic 304 steel reported in [15]. Such studies on TWIP are rare.

This article presents the continuation of our study on the strain rate sensitivity and strain hardening rate sensitivity of TWIP steels reported in Ref. [16]. It was shown that increasing the deformation rate leads to the reduction of the flow stress at given strain. This was associated with an inverse dependence of the strain hardening rate on the strain rate which, in turn, is caused by lower twin nucleation rate at high strain rates. The effect is associated

* Corresponding author.
E-mail address: picuc@rpi.edu (A.B. Lopes).

http://dx.doi.org/10.1016/j.msea.2016.07.127
0921-5093/

with the time dependence of the twin nucleation and growth processes which, although in principle weak, manifests itself in this case. Similar observations of the strain rate dependence of the twin density are reported in [17]. Here we extend this work investigating the local response of the material to nano- and micro-indentation. We observe that the local behavior is quite different from the global response: the material pre-deformed at high strain rates has higher nano-hardness than the material deformed at low strain rates. The presence of twins in the region of indentation leads to a softer elastic-plastic response. In micro-indentation tests the effective hardness of samples pre-deformed at higher strain rates decreases gradually and falls below the hardness of samples pre-deformed at low strain rates as the indenter size, and hence the probed volume of material, increase. We interpret the observation as a manifestation of the dual effect twins have on plasticity.

2. Material and experimental details

The nominal chemical composition of the TWIP steel used in this work is reported in Table 1. The high concentration of Mn stabilizes the austenitic phase at room temperature, whereas Si is added to prevent C precipitation. Samples were cut from sheets of 1.85 mm thickness supplied by POSCO Mill (South Korea).

Uniaxial monotonic tests were performed in tension at room temperature using a Shimadzu Autograph Machine (Schimadzu Japan) with maximum load capacity of 50kN. The equipment was coupled with a video extensometer Messphysik ME 46 (Austria). Tensile dog-bone shape specimens were cut parallel to the sheet rolling direction. Two strain rates were used: $10^{-4}\,s^{-1}$ and $0.47\,s^{-1}$. Vickers hardness measurements were carried out on samples deformed up to 20% strain at these two strain rates (separate samples), using a Shimadzu 2000-Vickers Instrument. A force of 4.9 N was applied for a duration of 10 s. Rockwell hardness (HRC) was also measured on same samples using a Karl Frank GMBH Frankoskop 38,180 hardness tester.

The SRS was evaluated from monotonic tensile tests performed with the two strain rates specified above: $10^{-4}\,s^{-1}$ and $0.47\,s^{-1}$. The SRS parameter was computed as $m = \log(\sigma_1/\sigma_2)/\log(\dot{\varepsilon}_1/\dot{\varepsilon}_2)$, where σ_1 and σ_2 are the values of the flow stress measured at given strain in tests performed with strain rates $\dot{\varepsilon}_1$ and $\dot{\varepsilon}_2$, respectively.

Nano-indentation tests were performed using a three-sided pyramidal Berkovich diamond indenter having a nominal tip radius of 20 nm, attached to a nano-indenter (TTX-NHT, CSM Instruments) and working in load control mode. Multiple arrays of 20×20 indents spaced 4 μm apart were performed by applying a maximum force of 7 mN. Some tests were performed with higher indentation loads, as specified below. All tests, including the pre-deformation, were performed at room temperature.

The microstructure was characterized using Scanning Electron Microscopy (SEM), Electron Backscattered Diffraction (EBSD) and Transmission Electron Microscopy (TEM). A HR-FESEM Hitachi SU70 equipment operating at 20 kV and endowed with a Quantax Cryst Align EBSD system from Bruker was used. The grains were identified based on the crystallographic direction parallel to the sample normal. Microstructural characterization was carried out after classical metallographic sample preparation, which included mechanical grinding and polishing followed by electro polishing using a Struers A2 electrolyte. The process was carried out in a Struers LectroPol-5 automatic electrolytic polishing and etching equipment operated at 35 V. The dislocation structures were observed with a Hitachi H-9000 (300 kV) transmission electron microscope (TEM). TEM foils oriented parallel to the rolling plane were taken at the sheet mid-thickness location. The samples were mechanically ground on both surfaces, then electropolished using a double-jet thinner (Struers Tenupol-3) with a solution of 5% perchloric acid in 95% acetic acid at 35 V, 0.5 A at room temperature (using a water cooling system) until perforation occurred.

Table 1
Chemical composition of the tested steel.

C	Mn	Si	Al	Fe
0.6%	18%	0.22%	1.5%	balance

3. Results and discussion

Fig. 1 shows the true stress-true strain curves corresponding to strain rates $10^{-4}\,s^{-1}$ and $0.47\,s^{-1}$. The yield stress measured at the two rates is approximately identical ($\sim$550 MPa). Strain hardening is more pronounced in samples deformed with the smaller strain rate and the difference between the small and large strain rate curves increases with strain. In [16–18] this behavior was associated with the higher twin nucleation rate in samples loaded at smaller strain rates. We also observe that samples loaded with smaller strain rates have larger strains at failure and, since strain hardening is almost strain-independent, larger ultimate tensile strength.

The strain rate sensitivity parameter (m) at yield is close to zero. Fig. 2 shows the variation of m with the true strain. The parameter was computed from the constant strain rate curves in Fig. 1. Similar values are reported in [16] from strain rate jump tests and for the same material. m decreases as the strain increases. At the strain of 20%, which is the pre-deformation strain applied to samples subjected to indentation in the present study, m is clearly negative.

To substantiate the dependence of the twin density on the strain rate, Fig. 3 shows TEM micrographs of two samples deformed to 20% strain at strain rates of $10^{-4}\,s^{-1}$ (Fig. 3(a)) and $0.47\,s^{-1}$ (Fig. 3(b)). The dislocation density is high, but approximately identical in the two cases. Most twins appear as plates of thickness smaller than $\sim$20 nm. Thicker twins are also observed but their number is smaller. Some twins run across entire grains, while others end inside the grains. The thicker twins tend to run across grains, which is expected due to the high energy associated with placing a twin tip within a crystal. The sample deformed slower has a larger twin density compared with the sample deformed faster. We evaluated the twin number density to be $\sim$72/μm^2 in the sample deformed with the higher strain rate and $\sim$100/μm^2 in the sample deformed with the lower strain rate,

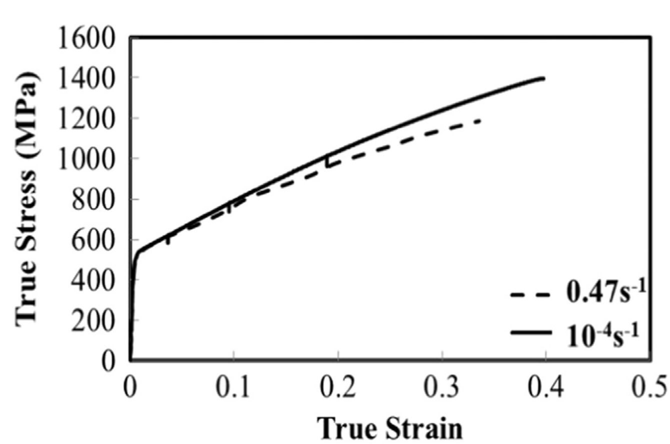

Fig. 1. True stress-true strain curves corresponding to the two strain rates indicated.